T-grafting BODIPY-Based Photosensitizers: The Synthesis of 2,6-Diethylacrylic-8-(*o*-methoxyphenyl)BODIPY and Its DSSC Performance

Reinner Ishaq Lerrick[1*], Wastiana Bere[1], Meliana Da Silva Braga[1], Agus Supriyanto[2], and Ali Hashem Essa[3]

[1]*Department of Chemistry, Faculty of Science and Engineering, University of Nusa Cendana, Jl. Adi Sucipto, Penfui-Kupang 85118, NTT, Indonesia*

[2]*Department of Physics, Faculty of Mathematics and Natural Sciences, Universitas Sebelas Maret, Jl. Ir. Sutami 36A, Kentingan, Surakarta 57126, Indonesia*

[3]*Department of Chemistry, College of Science, University of Basrah, Basrah 61004, Iraq*

** **Corresponding author:***

tel: +62-8113837791
email: reinner_lerrick@staf.undana.ac.id

Received: August 7, 2022
Accepted: November 22, 2022

DOI: 10.22146/ijc.76919

Abstract: *A new T-grafting photosensitizer of Dye-Sensitized Solar Cell (DSSC) has been developed by aligning Donor-Acceptor (D-A) group in an axially chiral BODIPY. Synthesis of the dye was conducted over a linear approach involving one-pot, non-oxidative synthesis of 1,3,5,7-tetramethyl-8-(o-methoxyphenyl)BODIPY, bromination, and finally C2/C6 ethyl acrylate Pd-Heck coupling to produce 65% of 2-ethylacrylic-1,3,5,7-tetramethyl-8-(o-methoxyphenyl)BODIPY (BOD-8) and 35% of 2,6-diethylacrylic-1,3,5,7-tetramethyl-8-(o-methoxyphenyl)BODIPY (BOD-9), both characterized by the appearance of acrylic alkenes at 6.05, and 7.63 ppm for BOD-8, and the additional 5.43, 7.80 ppm doublet peaks for BOD-9. The resulting dye showed excellent photon harvesting-related photovoltaic properties and electronic injection and regeneration processes where the acrylic esters were found to be the Donor and the aryl was the Acceptor. Eventually, the dye produced a current at 0.5% efficiency, similar to the horizontal D-A DSSC photosensitizer design.*

Keywords: *DSSC photosensitizer; T-grafted alignment; axially chiral BODIPY*

■ INTRODUCTION

BOron DiPyrromethanes (BODIPYs, (BOD-1), Fig. 1), 4,4-difluoro-4-bora-3a,4a-diaza-s-indacene an IUPAC name, are among the most versatile organic photoluminescence compound commonly applied in optoelectronic based organic semiconductors [1], chemical and biochemical sensors [2], molecular probes, photo dynamic therapy (PDT) [3] and Photo Thermal Therapy (PTT), and photo Acoustic Imaging (PAI) [4]. These facts are driven by their ease of accessible spectroscopic fine-tuned properties through the structure derivatizations, high photophysical properties, and high stabilities.

Recently, we developed axially chiral BODIPY (Ax*-BODIPY, (BOD-2)) from rotational-locked meso-aryl BODIPYs [5], those in which the perpendicular ortho-substituted phenyl moiety at C8 of the dipyrromethene core could not intramolecularly rotate, generating high quantum yield and longer lifetime rotor-based fluorophores for intracellular pH and viscosity sensing [6]. Meanwhile, the chemically distinguished acrylate group attached to the dipyrromethene proved to be a π-extended-based red-shift [7] and HOMO-LUMO band

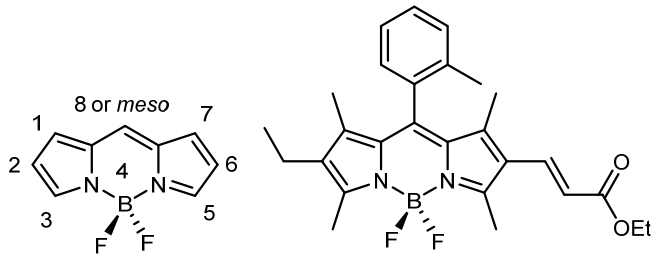

Fig 1. General structure and numbering of BODIPY (BOD-1) and Ax*-BODIPY developed (BOD-2)

gap (Eg) energy modifier due to its electron-withdrawing characteristic (EWG), and an anchoring group functioned essentially in Dye-Sensitized Solar Cell (DSSC) [8]. All these features allow for further organic photovoltaic (OPV) solar cell-related modifications of the molecules.

We, therefore, intend to employ further such orientation of the meso-aryl-lateral acrylate in the Ax*-BODIPY to design T-grafting DSSC photosensitizers (Fig. 2), a new Donor (D)-Acceptor (A) alignment on the BODIPY scaffold in which the aryl (proposed to be the D) at C8 and two acrylates (proposed to be the A) at C2 and C6, resembling that of current Akkaya's vertical (C8-D to C3 or C5-A), horizontal (C2-D to C-6-A), cross-conjugated BODIPY (C3, C5, and C7-D to C2-A) [9], and the pioneering Fukuzumi's D-A design [10], those which have been proven to increase the incident photon-to-current efficiency (IPCE) of the DSSC dyes.

■ EXPERIMENTAL SECTION

Materials

All the chemicals used in this research were obtained from Sigma Aldrich, TCI and Alfa Aesar in pure (99.9%) grade compounds. The solvents used in the reactions were dried, while the *n*-hexane (95% purity) used for column chromatography was re-distilled. The purification was done using silica gel column chromatography (flash, Kieselgel 60).

Instrumentation

The ^{1}H and ^{13}C-NMR spectra were obtained using 300.13 MHz and 75.47 MHz, respectively, on a Bruker Avance BVT3200 spectrometer, or 399.78 MHz and 100.53 MHz, respectively, using a Jeol JNM ECS400 spectrometer. The ^{19}F-NMR spectra were recorded at 376.17 MHz on a Jeol JNM ECS400 spectrometer. The Infrared analysis was performed using a Varian 800 FTIR Scimitar Series spectrometer scanning from 4000–600 cm^{-1}. The mass spectrometry analysis was done using a Micromass LCT Premier Mass Spectrometer in Electron Spray (ES) mode.

The UV-Vis and fluorescence spectra were recorded using a PerkinElmer Lamda 35 and DIGILAB HITACHI F-2500 FL spectrophotometer, respectively. The slit width was 2.5 nm for both excitation and emission. The DSSC solar cell performances were measured using Keithey type 2400A sourcemeter in the I-V parameter.

Procedure

Synthesis of 1,3,5,7-tetramethyl-8-(o-methoxyfenyl) BODIPY (BOD-4)

To a 50 mL round bottom flask was added 2-methoxybenzoylchloride (0.179 g, 1 mmol), DCM (25 mL) and 2,4-dimethylpyrrole (0.190 g, 2 mmol)

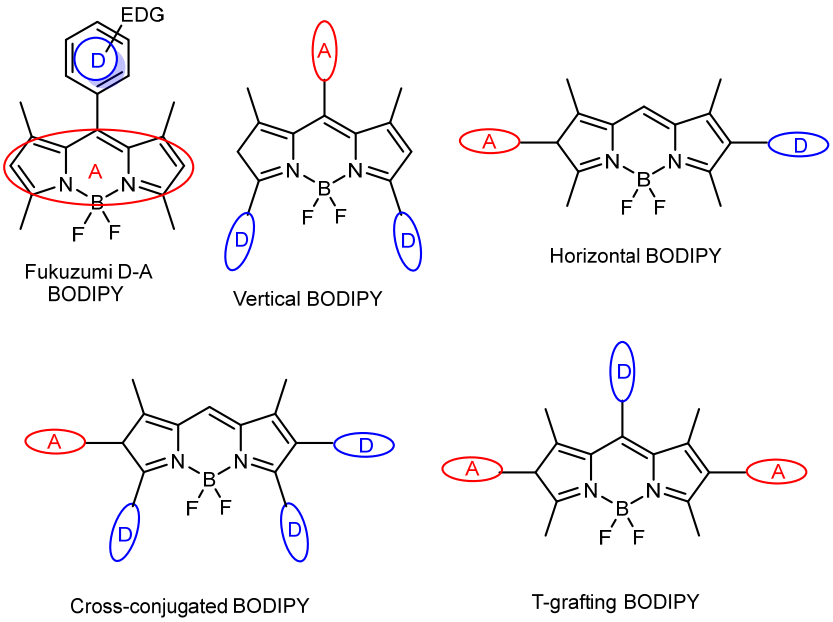

Fig 2. General type of D-A alignment on BODIPYs and the intent T-shape DSSC dye

sequentially. The solution was stirred overnight at room temperature under a nitrogen atmosphere. A 1 mL of *N*, *N*-diisopropyl-*N*-ethylamine was slowly added to the solution over 5 min, followed by 1 mL of $BF_3{\cdot}Et_2O$ at 0 °C. The solution was further stirred for 3 h. The solution was washed with 2 × 25 mL of water and dried using $MgSO_4$. The solvent was removed under reduced pressure to yield a dark brown solid residue. The crude product was then purified through column chromatography (*n*-hexane: ether = 15:1) to obtain an orange solid (BOD-4), 0.088 g (25%). R_f: 0.33 (UV active, petrol 40/60:ether = 1:1), m.p. = 242–243 °C, ^{1}H-NMR (300 MHz, $CDCl_3$): δ_H 1.45 (s, 6H, 2 Pyrrole C**H**$_3$), 2.57 (s, 6H, 2 Pyrrole C**H**$_3$), 3.79 (s, 3H, C**H**$_3$), 5.98 (s, 2H, 2 Pyrrole **H**), 7.00 (dd, *J* = 8.4, 0.9 Hz, 1H, Ar**H**), 7.09 (td, *J* = 7.3, 0.9 Hz, 1H, Ar**H**), 7.15 (dd, *J* = 7.4, 2.1 Hz, 1H, Ar**H**), 7.46 (ddd, *J* = 8.3, 7.2, 2.1 Hz, 1H, Ar**H**), ^{13}C-NMR, (100 MHz, $CDCl_3$): δ_C 13.8 (2 Pyrrole **C**H$_3$), 14.6 (2 Pyrrole **C**H$_3$), 55.6 (O**C**H$_3$), 111.1 (2 Pyrrole **C**H), 120.8 (Ar**C**H), 121.4 (Ar**C**H), 123.9 (2 Pyrrole **C**), 129.5 (Ar**C**H), 130.6 (Ar**C**H), 131.6 (Ar**C**), 139.0 (2 Pyrrole **C**-CH$_3$), 142.6 (2 Pyrrole **C**-CH$_3$), 154.9 (**C**$_{meso}$), 156.4 (Ar**C**-OCH$_3$), ^{19}F-NMR (376 MHz, $CDCl_3$): $J(^{19}F_A\text{-}^{11}B)$ = 33.7 Hz, $J(^{19}F_B\text{-}^{11}B)$ = 32.8 Hz, $J(^{19}F_A\text{-}^{19}F_B)$ = 110.7 Hz, IR(neat): ν_{max}/cm^{-1} 2980.9, 1540.0, 1505.3, 1463.0, 1307.0, 1187.6, 1156.6, 971.2, HRMS: calcd. for $C_{20}H_{22}BF_2N_2O$ $(M+H)^+$: 355.1788, found 355.1792.

Synthesis of 2-bromo-(BOD-5) and 2,6-dibromo-1,3,5,7-tetramethyl-8-(o-methoxyphenyl)BODIPY (BOD-6)

BOD-4 (0.285 g, 0.8 mmol), DCM (300 mL) and bromine (16.35 µL, 0.8 mmol) was added to a round bottom flask sequentially. The solution was stirred for 48 h at room temperature under a nitrogen atmosphere. The solution was washed with 2 × 25 mL of water and dried using $MgSO_4$. The remaining solvent was removed under reduced pressure to obtain a solid brown residue. The crude product was then purified through column chromatography (*n*-hexane:ether = 15:1) to give red solid (BOD-5), 0.190 g (55%) and (BOD-6). 0.190 g (46%).

BOD-5. R_f: 0.40 (UV active, petrol 40/60:ether = 7:3), m.p. = 204–206 °C, ^{1}H-NMR (300 MHz, $CDCl_3$): δ_H 1.44 (s, 3H, Pyrrole C**H**$_3$), 1.45 (s, 3H, Pyrrole C**H**$_3$), 2.58 (s, 3H, Pyrrole C**H**$_3$), 2.61 (s, 3H, Pyrrole C**H**$_3$), 3.79 (s, 3H, OC**H**$_3$), 6.03 (s, 1H, Pyrrole C**H**), 7.02 (d, *J* = 8.4 Hz, 1H, Ar**H**), 7.06–7.14 (m, 2H, 2 Ar**H**), 7.48 (ddd, *J* = 8.3, 6.3, 2.9 Hz, 1H, Ar**H**), ^{13}C-NMR, (100 MHz, $CDCl_3$): δ_C 12.8 (Pyrrole **C**H$_3$), 13.5 (Pyrrole **C**H$_3$), 13.9 (Pyrrole **C**H$_3$), 14.7 (Pyrrole **C**H$_3$), 55.6 (O**C**H$_3$), 110.3 (Pyrrole **C**-Br), 111.2 (Pyrrole **C**H), 121.6 (Ar**C**H), 121.7 (Pyrrole **C**-CH$_3$), 123.4 (Unbrominated pyrrole **C**-C$_{meso}$), 129.3 (Ar**C**H), 129.9 (Pyrrole **C**-CH$_3$), 130.9 (Ar**C**H), 132.2 (Ar**C**), 138.1 (Ar**C**H), 139.2 (Pyrrole **C**-CH$_3$), 144.6 (Pyrrole **C**-CH$_3$), 150.8 (Brominated pyrrole **C**-C$_{meso}$), 156.2 (**C**$_{meso}$), 157.4 (Ar**C**-OCH$_3$), ^{19}F-NMR (376 MHz, $CDCl_3$): $J(^{19}F_A\text{-}^{11}B)$ = 32.5 Hz, $J(^{19}F_B\text{-}^{11}B)$ = 31.8 Hz, $J(^{19}F_A\text{-}^{19}F_B)$ = 107.2 Hz, IR(neat): ν_{max}/cm^{-1} 2980.8, 1538.2, 1497.3, 1463.3, 1304.5, 1176.0, 1157.2, 975.8, 707.5, HRMS: calcd. for $C_{20}H_{21}BBrF_2N_2O$ $(M+H)^+$: 433.0893, found 433.0895.

BOD-6. R_f: 0.54 (UV active, petrol 40/60:ether = 7:3), m.p. = 231–233 °C, ^{1}H-NMR (300 MHz, $CDCl_3$): δ_H 1.44 (s, 6H, 2 Pyrrole C**H**$_3$), 2.62 (s, 6H, 2 Pyrrole C**H**$_3$), 3.79 (s, 3H, OC**H**$_3$), 7.03 (d, *J* = 8.3 Hz, 1H, Ar**H**), 7.10–7.14 (m, 2H, 2 Ar**H**), 7.51 (ddd, *J* = 8.3, 5.8, 3.4 Hz, 1H, Ar**H**), ^{13}C-NMR, (100 MHz, $CDCl_3$): δ_C 13.0 (2 Pyrrole **C**H$_3$), 13.7 (2 Pyrrole **C**H$_3$), 55.7 (O**C**H$_3$), 100.0 (2 Pyrrole **C**-Br), 111.3 (Ar**C**H), 121.7 (Ar**C**H), 123.3 (2 Pyrrole **C**-CH$_3$), 129.2 (Ar**C**H), 130.6 (2 Pyrrole **C**-CH$_3$), 131.2 (Ar**C**H), 139.7 (Ar**C**), 140.2 (Pyrrole **C**-C$_{meso}$), 153.5 (**C**$_{meso}$), 156.4 (Ar**C**-OCH$_3$), IR(neat): ν_{max}/cm^{-1} 2924.5, 1541.3, 1460.6, 1401.2, 1350.0, 1178.5, 991.8, 756.5, HRMS: calcd. for $C_{20}H_{20}BBr_2F_2N_2O$ $(M+H)^+$: 512.9982, found 512.9977.

Synthesis of 2-bromo-6-ethylacrylaic-(BOD-8) and 2,6-diethylacrylaic-1,3,5,7-tetramethyl-8-(o-methoxy phenyl)BODIPY (BOD-9)

To a Schlenk tube was added (BOD-6) (175 mg g, 0.400 mmol), Pd(II) acetate (3 mg, 0.012 mmol), triphenylphosphine (7 mg, 0.028 mmol) and 5 mL DMF. The mixture was stirred for 10 min and followed by the addition of ethyl acrylate (92 mg, 0.922 mmol) and triethylamine (185 mg, 1.832 mmol) in DMF (7 mL). The solution was then warmed for 24 h. A 50 mL DCM was added to the solution and washed with 2 × 200 mL water. The organic phase was dried using $MgSO_4$, and the remaining solvent was removed under reduced pressure to yield a red solid residue. The crude product

was then purified through column chromatography (petrol 40/60:ether = 10:1) to give red solid (BOD-8), 0.137 g (64.6%) and (BOD-9), 0.077 (35%).

BOD-8. ^{1}H-NMR (300 MHz, $CDCl_3$): δ_H 1.32 (t, *J* = 7.1 Hz, 3H, C**H**$_3$), 1.44 (s, 3H, Pyrrole C**H**$_3$), 1.54 (s, 3H, Pyrrole C**H**$_3$), 2.64 (s, 3H, Pyrrole C**H**$_3$), 2.72 (s, 3H, Pyrrole C**H**$_3$), 3.79 (s, 3H, OC**H**$_3$), 4.24 (q, *J* = 7.1 Hz, 2H, C**H**$_2$), 6.05 (d, *J* = 16.2 Hz, 1H, C**H**), 6.06 (s, 1H, Pyrrole **H**), 7.02(d, *J* = 8.3 Hz, 1H, Ar**H**), 7.08–7.21 (m, 2H, 2 Ar**H**), 7.49 (ddd, *J* = 8.3, 5.2, 4.0 Hz, 1H, Ar**H**), 7.63 (d, *J* = 16.2 Hz, 1H, C**H**), ^{13}C-NMR, (100 MHz, $CDCl_3$): δ_C 11.9 (Br-substituted pyrrole **C**H$_3$), 13.9 (Br-substituted pyrrole **C**H$_3$), 14.2 (Acrylic CH$_2$**C**H$_3$), 14.4 (Substituted pyrrole **C**H$_3$), 14.9 (Substituted pyrrole **C**H$_3$), 55.6 (O**C**H$_3$), 60.2 (Acrylic **C**H$_2$CH$_3$), 99.3 (Br-substituted pyrrole **C**-Br), 111.2 (Ar**C**H), 117.1 (=**C**HCO and Br-substituted **C**-CH3), 121.6 (Ar**C**H), 122.4 (Br-substituted pyrrole **C**-C$_{meso}$), 123.6 (Br-substituted pyrrole **C**-CH$_3$), 129.4 (Ar**C**H), 130.7 (Substituted pyrrole **C**-CH), 130.9 (Ar**C**), 132.9 (**C**$_{meso}$), 135.9 (Ar**C**H and Substituted **C**-C$_{meso}$), 144.9 (=**C**H), 156.4 (2 Substituted pyrrole **C**-CH$_3$), 1587.0 (Ar**C**-OCH$_3$), 167.7 (Acrylic **C**=O).

BOD-9. ^{1}H-NMR (300 MHz, $CDCl_3$): δ_H 1.33 t, *J* = 7.1 Hz, 6H, 2 C**H**$_3$), 1.45 (s, 3H, Pyrrole C**H**$_3$), 1.54 (s, 3H, Pyrrole C**H**$_3$), 2.64 (s, 3H, Pyrrole C**H**$_3$), 2.72 (s, 3H, Pyrrole C**H**$_3$), 3.79 (s, 3H, OC**H**$_3$), 4.25 (q, *J* = 7.1 Hz, 4H, 2 C**H**$_2$), 5.43 (d, *J* = 16.3 Hz, 1H, C**H**), 6.06 (d, *J* = 16.3 Hz, 1H, C**H**), 6.08 (s, 1H, Ar**H**), 7.13–7.16 (m, 2H, 2 Ar**H**), 7.52 (ddd, *J* = 8.3, 5.6, 3.7 Hz, 1H, Ar**H**), 7.60 (d, *J* = 16.2 Hz, 1H, C**H**), 7.80 (d, *J* = 16.2 Hz, 1H, C**H**), ^{13}C-NMR, (100 MHz, $CDCl_3$): δ_C 11.4 (Pyrrole **C**H$_3$), 11.9 (Pyrrole **C**H$_3$), 14.5 (Pyrrole **C**H$_3$), 14.9 (2 Acrylic CH$_2$**C**H$_3$), 17.2 (Pyrrole **C**H$_3$), 55.2 (O**C**H$_3$), 60.3 (2 Acrylic **C**H$_2$CH$_3$), 111.3 (Ar**C**H and pyrrole **C**-CH), 116.6 (=**C**HCO), 121.7 (Ar**C**H and =**C**HCO), 122.4 (Pyrrole **C**-C$_{meso}$ and Ar**C**H), 123.9 (Pyrrole **C**-C$_{meso}$), 129.6 (Ar**C**H and pyrrole **C**CH), 130.7 (**C**$_{meso}$), 130.9 (Ar**C**), 136.4 (Ar**C**H), 143.0 (Pyrrole **C**-CH$_3$ and =CH), 144.9 (=**C**H and pyrrole **C**-CH$_3$), 156.6 (Ar**C**OCH$_3$), 167.8 (2 Acrylic **C**=O).

Spectroscopic measurement

The absorption properties of the BODIPYs were measured by scanning a serial concentration of the samples in organic solvent from 250–700 nm. A plot of concentration vs. absorption was made to produce a linear regression curve used to generate the extinction coefficient (ε). Meanwhile, the fluorescence quantum yield (φ) was determined over scanning of a series of the dilute sample within the absorbance range 0.01 < A < 0.05 followed by calculation through φ equation:

$$\varphi_{sample} = \varphi_{s\,tan\,dard} \times \frac{F_{sample}}{F_{s\,tan\,dard}} \times \frac{A_{s\,tan\,dard}}{A_{sample}} \times \left(\frac{n_{sample}}{n_{s\,tan\,dard}} \right)^2$$

where F stands for the area under the sample and standard emission spectrum, A is for the sample and standard absorbance, and n denotes the refractive index of the solvent used to dilute the sample and the standard. Here we used Rhodamine-B (φ = 0.70 in MeOH, λ_{ex} = 512 nm) and the well-known BOD-4 photophysics data (λ_{ex} = 485 nm) as the standard.

Computational calculation

All dyes were submitted to Gaussian 09 package to calculate their band gap energy (Eg) and the HOMO-LUMO model using the density functional theory (B3LYP) method with the SDD basis set level [11].

DSSC fabrication

A TiO_2 slurry in ethanol was leveled using the doctor Blade technique onto the 2.5 × 2.5 mm conductive surface of FTO glass to make a 2.0 × 2.0 mm working electrode. The electrode was sintered under 250 °C and left to cool at room temperature. A dye solution was then slowly dropped to the TiO_2 surface (ca. 13 μm) and was left to dry overnight at room temperature. Meanwhile, the carbon counter electrode was prepared by coating the conductive site of another 2.0 × 2.0 mm FTO glass with candle soot. The KI/I_2 electrolyte was dropped onto the working electrode, and the counter electrode was then covered to make a sandwich-like DSCC cell.

I-V measurement

The organic photovoltaic (OPV) performances were measured using 2602A Keithley under adjusted 1000 Watt/m^2 of xenon lamp illumination and non-illumination (Dark condition) of the fabricated cells, and all were at room temperature.

■ RESULTS AND DISCUSSION

Synthesis of 2,6-Dietylacrilaic-8-(*o*-methoxyphenyl) BODIPY

To access the desired T-grafting BODIPYs, we opted to introduce the *o*-methoxyphenyl group as the Donor unit [12] at C8 due to its effective electron-hole separation upon photoexcitation of the dyes leading to electron current injection to the TiO_2 conduction band [18] and its biocompatibility [13], one of the required photosensitizer properties due to the typical low light energy conversion efficiency (η)-ascribed dyes aggregation on the TiO_2 surface [9]. Accordingly, we submitted *o*-methoxybenzoylchloride to 2,4-dimethylpyrrole (3) in the presence of Grignard reagent as a base catalyst following modified Sunahara's procedure [14] (Fig. 3). This one-pot non-oxidative in-situ dipyrromethene production was followed by adding Hüning's amine and $BF_3{\cdot}OEt_2$ to obtain an orange solid in 25% yield confirmed spectroscopically as (BOD-4) based on Sunahara's ^1H and ^{13}C-NMR [14] spectra agreement.

Furthermore, the intent high emission-driven rotational lock *meso*-aryl substituent design was asserted by the appearance of two double-quartet (dq) AMX splitting patterns ascribed to the two quartets (q) 33.7 and 32.8 Hz of ^{11}B-^{19}F and one double 110.8 Hz of ^{19}F-^{19}F coupling (Fig. 4).

The next step was to halogenate the BODIPY (BOD-4). As the C2/C6 is the only available position, such bromine (Br_2) addition would then produce the desired

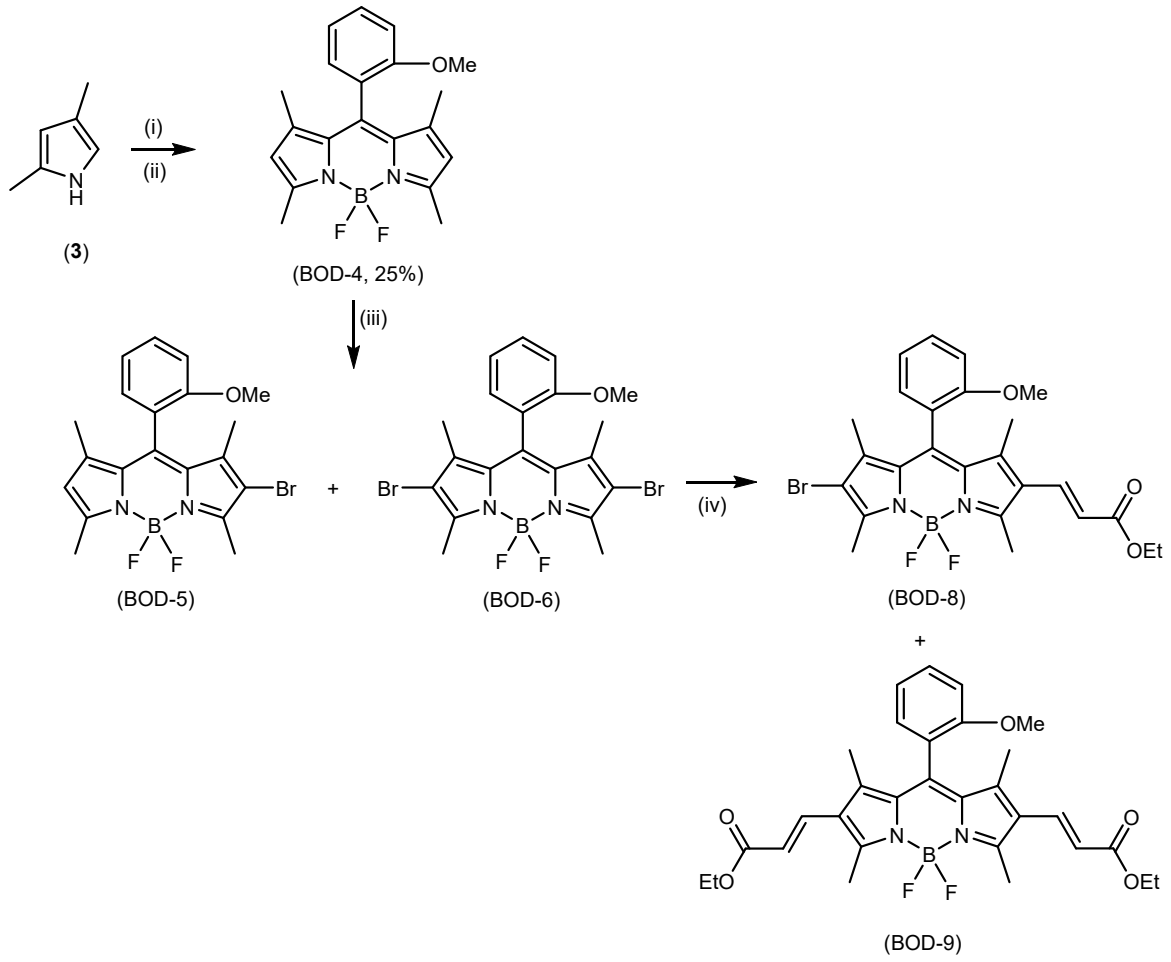

(i) 2-methoxybenzoylchlroide, PhMgBr, DCM, r.t., over night; (ii) *N*,*N*-diisopropyl-*N*-etylamine, BF_3OEt_2, 0 °C, 3 h, r.t.; (iii) Br_2, DCM, r.t., 48 h; (iv) ethyl acrylate, Pd(OAc)2, PPh3, DMF, triethylamine, 24 h

Fig 3. Synthesis of (BOD-9)

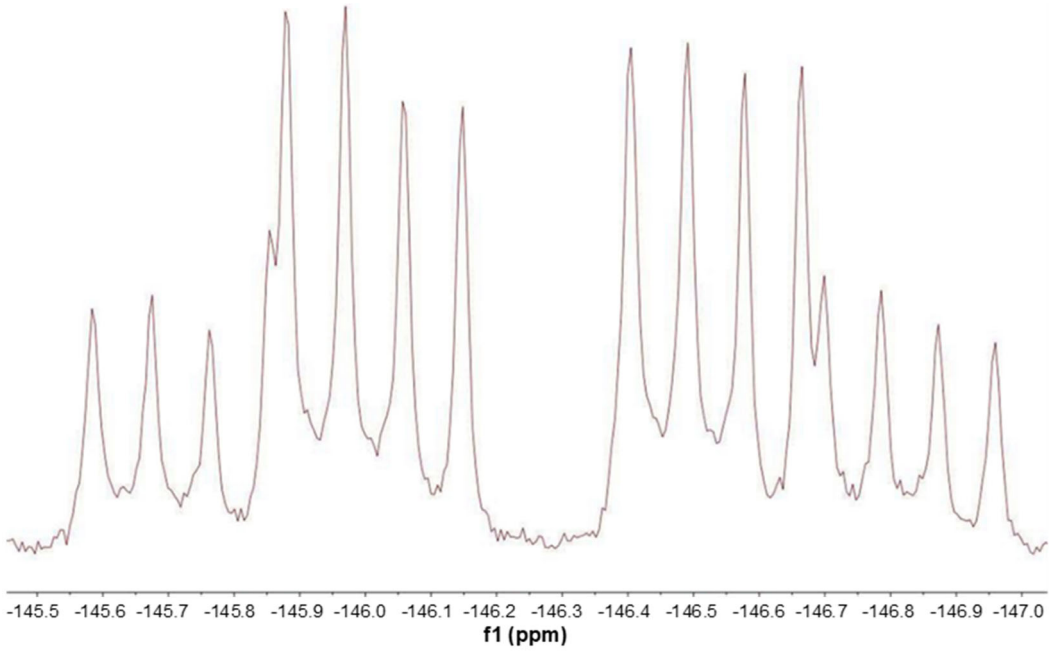

Fig 4. ^{19}F-NMR spectrum of (BOD-4)

halogenated BODIPY, a required precursor for the late-stage Heck coupling reaction using ethyl acrylate (Fig. 3). Thereby, submission of bromine into the solution of (BOD-4) in DCM produced two separable red solids, which spectroscopically proved to be mono (BOD-5) and dibrominated (BOD-6) product in referring to its singlet, one pyrrole proton peak at 6.03 ppm and no pyrrole peak at ~6 ppm, respectively (see Supplementary Information, SI). The method is even mole ratio control, where the optimum dibromination was achieved at a 1:2 mole ratio (Table 1 entry 4).

Finally, conducting a facile, high-yield, and straightforward palladium Heck coupling reaction of (BOD-6) to the mixture of ethyl acrylate in DMF produced two red solids, beneficially catalyst-based reaction control (Table 2). The ^{1}H-NMR spectrum analysis for those two products showed one typical alkenes doublet (d) 'roofing' AA′ pattern at 6.05 and 7.63 ppm (J = 16.2 Hz) corresponding to mono acrylated (BOD-8) and another additional one at 5.43 and 7.60 ppm (J = 16.3 Hz) confirming the desired product (BOD-9), along with the ester's -CH_3 at 1.33 ppm (t, J = 7.1 Hz) and -CH_2- group at 4.25 ppm (q, J = 7.1 Hz) at both products (see SI).

Table 1. Mole ratio control of bromination reaction of (BOD-4)

Entry	Ratio (BOD-4) to Br_2	Time (h)	Yield (BOD-5):(BOD-6)(%)
1	1:1	24	40:20
2	1:1	48	55:46
3	1:1.1	48	44:45
4	1:2	24	20:80

Table 2. Optimization of Heck coupling of (BOD-6) with ethyl acrylate

Entry	Pd^{2+} (mol%)	PPh_3 (mol%)	Time (h)	Yield (BOD-8):(BOD-9)(%)
1	3	7	24	65:35
2	3.5	7	24	30:70

Photophysical and Electrochemical Properties and Photovoltaic Performance

Before employing the BODIPYs as the DSSC photosensitizers, the incident photon-to-current efficiency (IPCE)-related photophysics and electrochemical properties of those synthesized BODIPYs were evaluated to ensure that the designed dyes work correctly. As shown in Fig. 5, all BODIPYs gave typical BODIPYs' 0-1 vibronic signature spectrum [9], a so-called 'shoulder' due to $S_0 \rightarrow S_2$ electronic transition and weaker $S_0 \rightarrow S_n$ ($n \geq 2$) bands at shorter wavelength [11] which exhibited a Batochromic effect as their π-extended C2/C6 modification [15], the desired effect in optimizing the absorption of mainly Near Infra-Red (NIR) spectrum of the sun by the dyes [10,19]. Meanwhile, the increase of the relative area of those BOD-8 and BOD-9 $S_0 \rightarrow S_1$ bands to that of the unsubstituted BOD-4 indicates proportionally the mono- and the di- β-substituted, respectively [16]. All the fluorophores' fluorescence spectra were also a mirror image of that of the absorption.

As predicted, the BOD-4 gave typical high absorptivity, narrow Stokes shift ($\lambda_{Em} - \lambda_{Abs} = 10$ nm), and high φ (up to 90%), BODIPYs' typical photophysics [11], ascribed from the effective non-radiative relaxation blocked at the aryl *meso* functional group (Table 1, entry 1). The red-shift absorption and emission found in both the brominated BOD-5 (12 nm) and BOD-6 (27 nm) (Table 3, entry 2 and 3) and the ethyl acrylate substituted BOD-8 (40 nm) and BOD-9 (52 nm) corresponds to the Inter-system Crossing (ISC) process over the heavy atom effect, also proven by the drastic decrease of their quantum yield, and the π-extended effect, respectively. The rotational restriction of the orthogonal (*o*-methoxyphenyl) at C8 compensates substantially [17] for the Br heavy atom effect in BOD-8 as well as in the BOD-9 (Table 3, entry 4 and 5) resulted in exceptionally high φ.

As the photon harvesting-related photophysical properties of the dyes have satisfactorily been confirmed, we then conducted the electron injecting and regenerating-related electronic properties of the designed dyes, those two primary parameters in producing high ICPE. We then conducted DFT (B3LYP/SDD) calculation using the Gaussian 09 package of the dyes. Instead of laying on the intended *o*-methoxyphenyl donor group [16], we found that the electrons are otherwise delocalized mostly in the dipyrromethene ring (BOD-4 HOMO) and surprisingly in the excited state (LUMO), this *meso* orthogonal aryl group

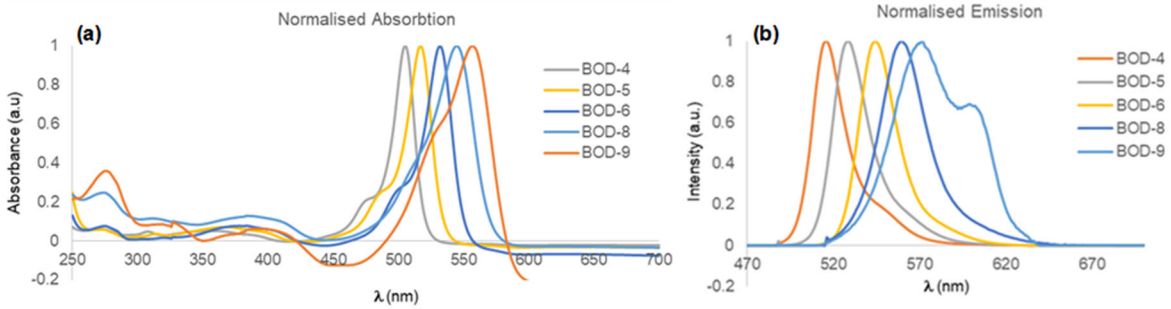

Fig 5. Absorption (a) and Emission spectra (b) of the prepared BODIPYs

Table 3. Optical density and fluorescence properties of the synthesized BODIPYs

Entry	Compound	ε (L mol^{-1} cm^{-1})	λ_{Abs} (nm)	λ_{Em} (nm)	φ
1	BOD-4	110,900	505[a]	515[a]	0.889[a]
2	BOD-5	70,000	517	528	0.17[b]
3	BOD-6	52,500	532	544	0.05[b]
4	BOD-8	72000	545	559	0.060[c]
5	BOD-9	92500	557	571	0.502[c]

[a]: reference [14] [b]: BOD-4 was the standard in DCM (λ_{ex} = 485 nm) [c]: Rhodamine-B was the standard in MeOH (φ = 0.70, λ_{ex} = 512 nm)

'pulls' the charge density through a mesomeric effect [11]. The effect commonly plays by acceptor groups (see SI). Similarly, the ethyl acrylate group (BOD-8 and BOD-9), expected to be the acceptor group over its π-extended 'pull' effect, is found to bear electron density in their ground state (HOMO) substantially and otherwise 'pushes' the electron to the *o*-methoxyphenyl [11], suitable to be a donor group (see SI). This reverse effect could plausibly cause by the use of the ester of acrylate instead of the acid one [18]. Thereby, our revised T-designed DSSC photosensitizer is like in Fig. 6.

Hitherto our photosensitizers are still found to comply with the electronic driving force requirement (Fig. 7). Those LUMO energies lie upper the TiO_2 conduction band (-4.2 eV) whist the HOMO levels are below then the electrolyte (I_3^-/I^-) redox potential (-5.2 eV), indicating efficient electron injection of the dyes upon photoexcitation to the TiO_2 and efficient dyes regeneration over the electrolyte-cationic dye redox process, respectively [9-10]. The 'push-pull'-related ethyl acrylate C2/C6 introduction effect has also been observed by the reduction of the dyes band gap (Eg) (Table 4), one of the recommended strategies in the high IPCE organic photovoltaic (OPV) design [20].

Finally, upon halogen lamp illumination to the fabricated DSSC cells, our dyes produced current (Fig. 8). Meanwhile, the T-grafted dye produced a 0.5% ratio of electrical power to the incident sunlight conversion (η) (Table 4 entry 4), similar to the horizontal D-A DSSC photosensitizers alignment. This achievement is much better than its corresponding D-A Fukuzumi-designed dyes [10].

Through these results, we have also seen the heavy atom-related quenching effect on the photosensitizing ability (Entry 1 and 2) and the significant contribution of the acrylate, as a donor, to resolve this effect found in BOD-8 (Entry 3).

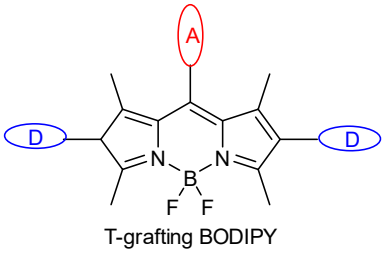

Fig 6. The revised T-grafting photosensitizer

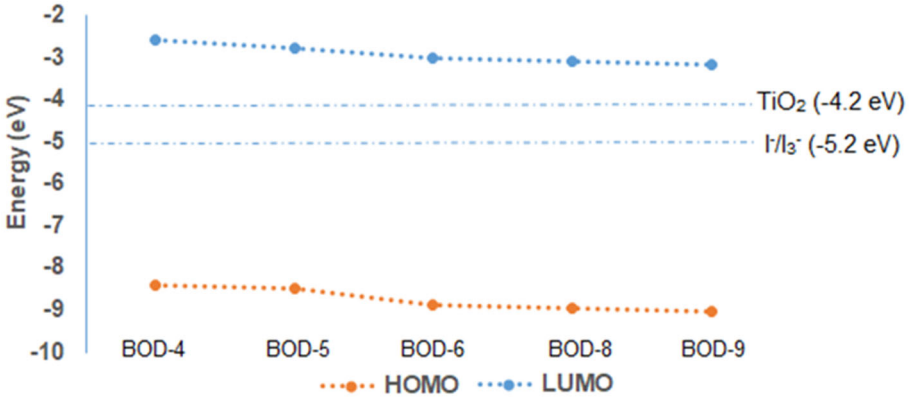

Fig 7. Energy level diagram of those synthesized BODIPY

Table 4. Photovoltaic properties of the prepared dyes

Entry	Dye	Eg (eV)	V_{oc} (mV)[a]	J_{sc} (mA cm^{-2})[b]	FF[c]	H (%)[d]	Dye amount (10^{-7} mol cm^{-2})
1	BOD-5	2.94	0.3333	0.000016	0.259	0.000354	0.1542
2	BOD-6	2.91	n.d.	n.d.	-	-	0.6536
3	BOD-8	2.80	0.075707	0.000116	0.277	0.000121	0.1634
4	BOD-9	2.74	0.1817	0.13240	0.517	0.497	0.6845

[a]: Open-circuit voltage, [b]: Short-circuit current, [c]: Fill factor, [d]: Power conversion efficiency, n.d.: not detected

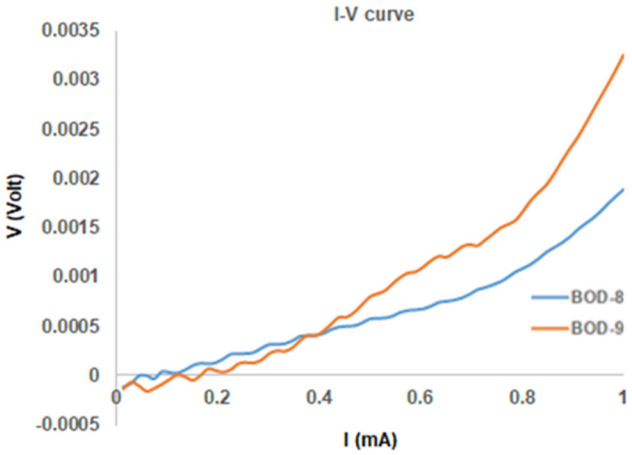

Fig 8. The I-V curve of the fabricated dye sensitizer

■ CONCLUSION

A new potent DSSC photosensitizer has been achieved by utilizing *meso*-substituted *o*-methoxyphenyl-1,3,5,7-tetramethyl BODIPY. Incorporating ethyl acrylate at C2/C6 of the BODIPY produced a T-grafting DSSC photosensitizer which was photophysical and electronic satisfactorily in conducting photovoltaic processes. The dye had typical horizontal D-A alignment current efficiency (η) of 0.5% in fabrication.

■ ACKNOWLEDGMENTS

The author(s) thank the Faculty of Science and Engineering, University of Nusa Cendana, for the research grant (Number: 16/UN15.15.2.PPK/SPP/FST/III/2022).

■ AUTHOR CONTRIBUTIONS

Reinner Ishaq Lerrick conducted the syntheses and the spectroscopy analysis and wrote this manuscript. Meliana Da Silva Braga and Wastiana Bere carried out the DSSC fabrications. Agus Supriyanto performed I-V measurements of the DSSCs. Ali Hashem Essa did the calculations for the DFT. All authors approved this manuscript's final version.

■ REFERENCES

[1] Squeo, B.M., Ganzer, L., Virgili, T., and Pasini, M., 2020, BODIPY-based molecules, a platform for photonic and solar cells, *Molecules*, 26 (1), 153.

[2] Saravanan, V., Ganesan, S., and Rajakumar, P., 2020, Synthesis and DSSC application of BODIPY decorated triazole bridged and benzene nucleus cored conjugated dendrimers, *RSC Adv.*, 10 (31), 18390–18399.

[3] Awuah, S.G., and You, Y., 2012, Boron dipyrromethene (BODIPY)-based photosensitizers for photodynamic therapy, *RSC Adv.*, 2 (30), 11169–11183.

[4] Merkes, J.M., Lammers, T., Kancherla, R., Rueping, M., Kiessling, F., and Banala, S., 2020, Tuning optical properties of BODIPY dyes by pyrrole conjugation for photoacoustic imaging, *Adv. Opt. Mater.*, 8 (11), 1902115.

[5] Lerrick, R.I., Winstanley, T.P.L., Haggerty, K., Wills, C., Clegg, W., Harrington, R.W., Bultinck, P., Herrebout, W., Benniston, A.C., and Hall, M.J., 2014, Axially chiral BODIPYs, *Chem. Commun.*, 50 (36), 4714–4716.

[6] Radunz, S., Kraus, W., Bischoff, F.A., Emmerling, F., Tschiche, H.R., and Resch-Genger, U., 2020, Temperature- and structure-dependent optical properties and photophysics of BODIPY dyes, *J. Phys. Chem. A*, 124 (9), 1787–1797.

[7] Feng, Z., Jiao, L., Feng, Y., Yu, C., Chen, N., Wei, Y., Mu, X., and Hao, E., 2016, Regioselective and stepwise syntheses of functionalized BODIPY dyes through palladium-catalyzed cross-coupling reactions and direct C-H arylations, *J. Org. Chem.*, 81 (15), 6281–6291.

[8] Klfout, H., Stewart, A., Elkhalifa, M., and He, H., 2017, BODIPYs for dye-sensitized solar cells, *ACS Appl. Mater. Interfaces*, 9 (46), 39873–39889.

[9] Shah, M.F., Mirloup, A., Chowdhury, T.H., Sutter, A., Hanbazazah, A.S., Ahmed, A., Lee, J.J., Abdel-Shakour, M., Leclerc, N., Kaneko, R., and Islam, A., 2020, Cross-conjugated BODIPY pigment for highly efficient dye sensitized solar cells, *Sustainable Energy Fuels*, 4 (4), 1908–1914.

[10] Mao, M., and Song, Q.H., 2016, The structure-property relationships of D-π-A BODIPY dyes for dye-sensitized solar cells, *Chem. Rec.*, 16 (2), 719–733.

[11] Lu, H., Mack, J., Yang, Y., and Shen, Z., 2014, Structural modification strategies for the rational design of red/NIR region BODIPYs, *Chem. Soc. Rev.*, 43 (13), 4778–4823.

[12] Hosseinnezhad, M., Gharanjig, K., and Moradian, S., 2020, New D–A–π–A organic photo-sensitizer with thioindoxyl group for efficient dye-sensitized solar cells, *Chem. Pap.*, 74 (5), 1487–1494.

[13] Liu, M., Ma, S., She, M., Chen, J., Wang, Z., Liu, P., Zhang, S., and Li, J., 2019, Structural modification of BODIPY: Improve its applicability, *Chin. Chem. Lett.*, 30 (10), 1815–1824.

[14] Sunahara, H., Urano, Y., Kojima, H., and Nagano, T., 2007, Design and synthesis of a library of BODIPY-based environmental polarity sensors utilizing photoinduced electron-transfer-controlled fluorescence ON/OFF switching, *J. Am. Chem. Soc.*, 129 (17), 5597–5604.

[15] Ren, W., Xiang, H., Peng, C., Musha, Z., Chen, J., Li, X., Huang, R., and Hu, Y., 2018, Direct C-H functionalization of difluoroboron dipyrromethenes (BODIPYs) at β-position by iodonium salts, *RSC Adv.*, 8 (10), 5542–5549.

[16] Chen, J., Mizumura, M., Shinokubo, H., and Osuka, A., 2009, Functionalization of boron dipyrrin (BODIPY) dyes through iridium and rhodium catalysis: A complementary approach to α-and β-substituted BODIPYs, *Chem. - Eur. J.*, 15 (24), 5942–5949.

[17] Farfán-Paredes, M., González-Antonio, O., Tahuilan-Anguiano, D.E., Peón, J., Ariza, A., Lacroix, P.G., Santillan, R., and Farfán, N., 2020, Physicochemical and computational insight of ^{19}F NMR and emission properties of *meso*-(*o*-aryl)-BODIPYs, *New J. Chem.*, 44 (45), 19459–19471.

[18] Hattori, S., Ohkubo, K., Urano, Y., Sunahara, H., Nagano, T., Wada, Y., Tkachenko, N.V., Lemmetyinen, H., and Fukuzumi, S., 2005, Charge separation in a nonfluorescent donor-acceptor dyad derived from boron dipyrromethene dye, leading to photocurrent generation, *J. Phys. Chem. B*, 109 (32), 15368–15375.

[19] Cui, Y., Yao, H., Zhang, J., Zhang, T., Wang, Y., Hong, L., Xian, K., Xu, B., Zhang, S., Peng, J., Wei, Z., Gao, F., and Hou, J., 2019, Over 16% efficiency organic photovoltaic cells enabled by a chlorinated acceptor with increased open-circuit voltages, *Nat. Commun.*, 10 (1), 2515.

[20] Bessette, A., and Hanan, G.S., 2014, Design, synthesis and photophysical studies of dipyrromethene-based materials: Insights into their applications in organic photovoltaic devices, *Chem. Soc. Rev.*, 43 (10), 3342–3405.

Supplementary Data

This supplementary data is a part of a paper entitled "T-grafting BODIPY-Based Photosensitizers: The Synthesis of 2,6-Diethylacrylic-8-(*o*-methoxyphenyl)BODIPY and Its DSSC Performance".

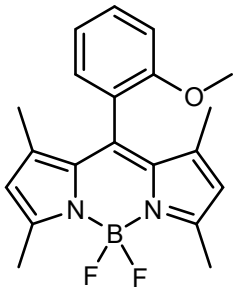

(BOD-4)

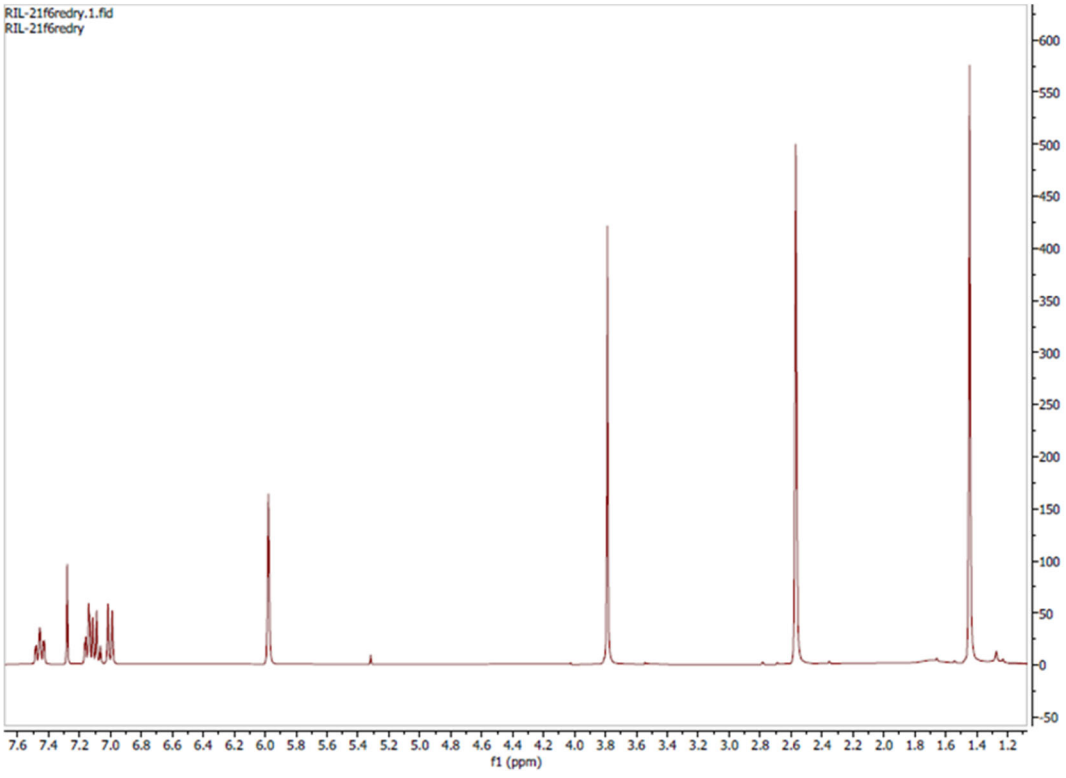

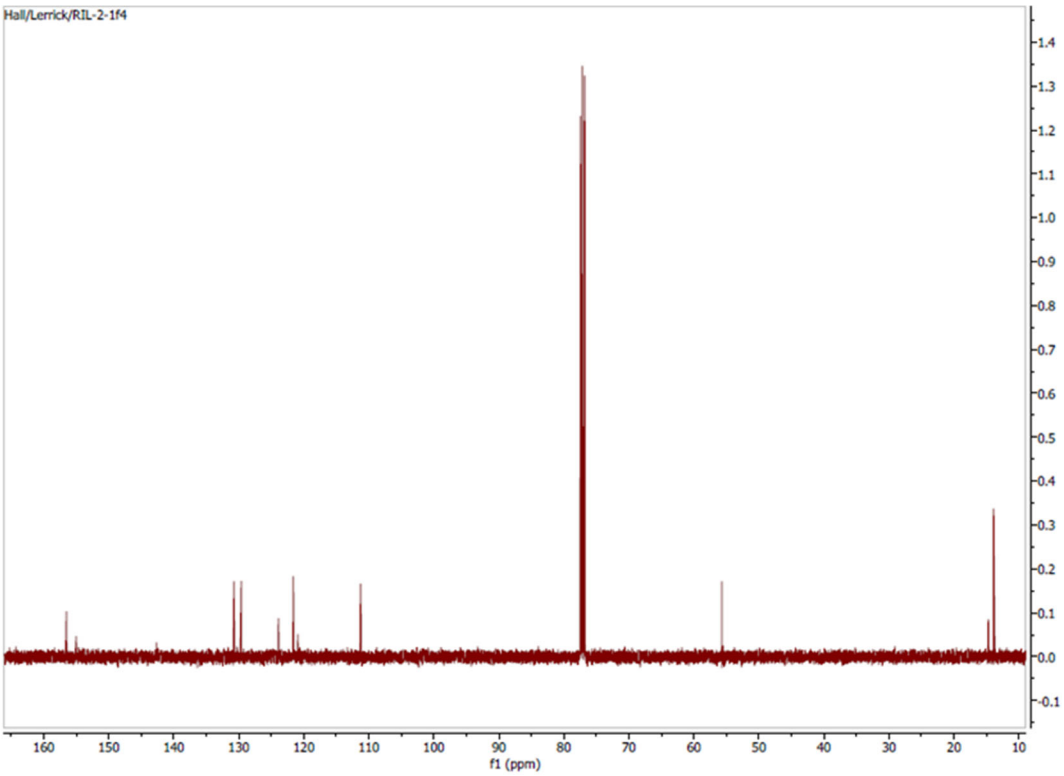
Hall/Lerrick/RIL-2-1f4
f1 (ppm)

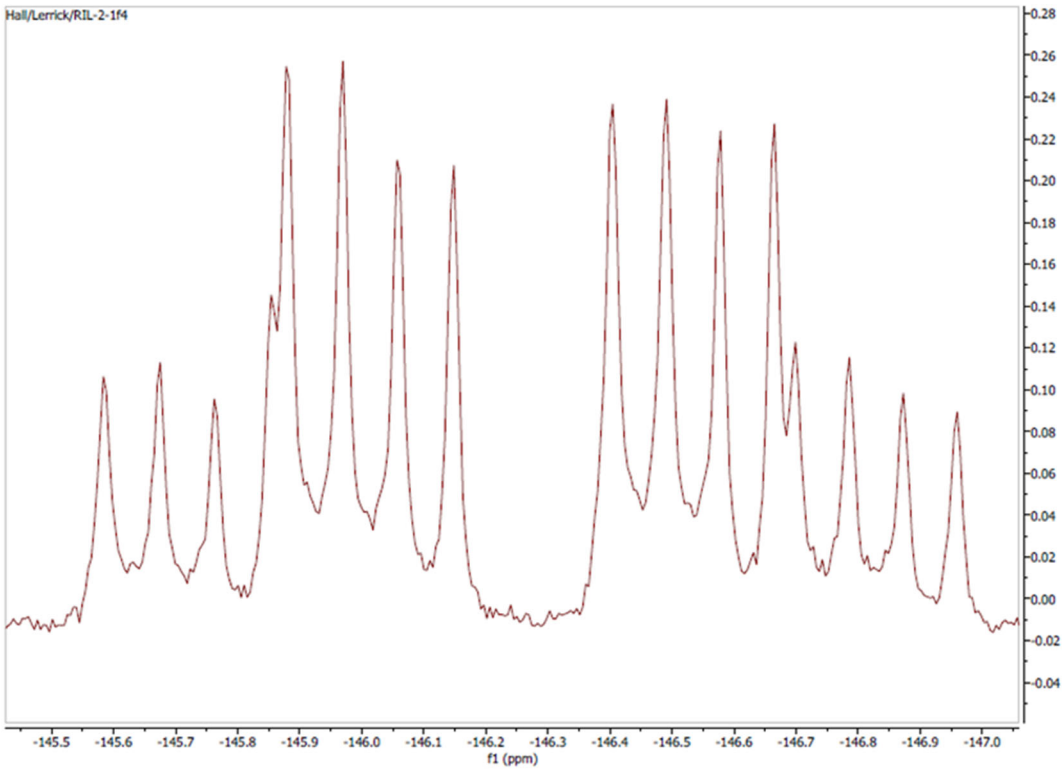
Hall/Lerrick/RIL-2-1f4
f1 (ppm)

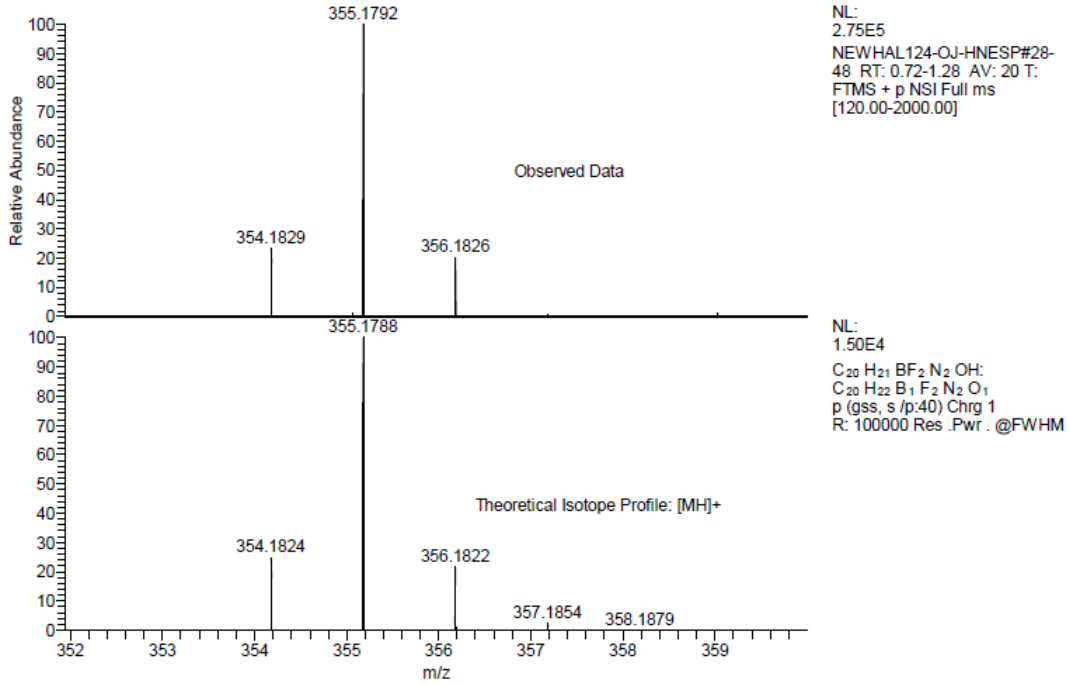
355.1792
NL:
2.75E5
NEWHAL124-OJ-HNESP#28-48 RT: 0.72-1.28 AV: 20 T: FTMS + p NSI Full ms [120.00-2000.00]
Observed Data
354.1829
356.1826
Relative Abundance
355.1788
NL:
1.50E4
C20 H21 BF2 N2 OH:
C20 H22 B1 F2 N2 O1
p (gss, s /p:40) Chrg 1
R: 100000 Res .Pwr . @FWHM
Theoretical Isotope Profile: [MH]+
354.1824
356.1822
357.1854
358.1879
m/z

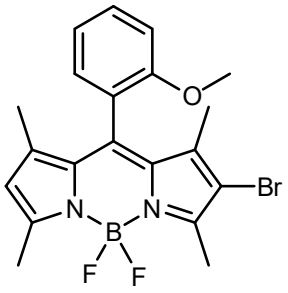

(BOD-5)

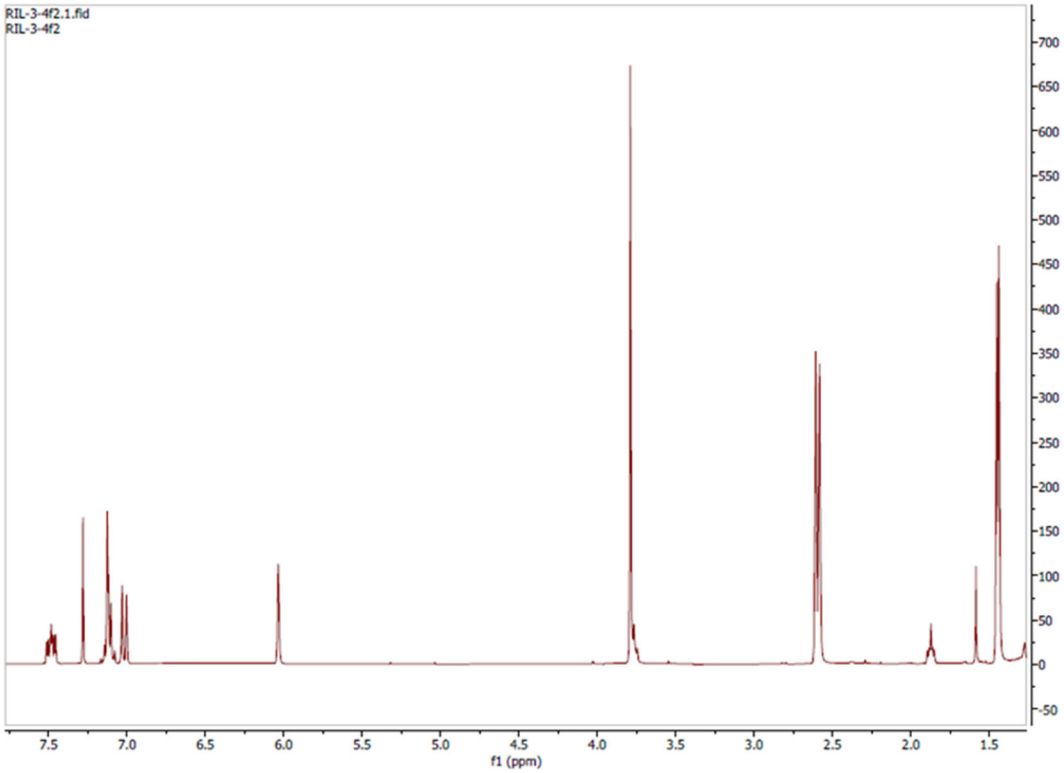

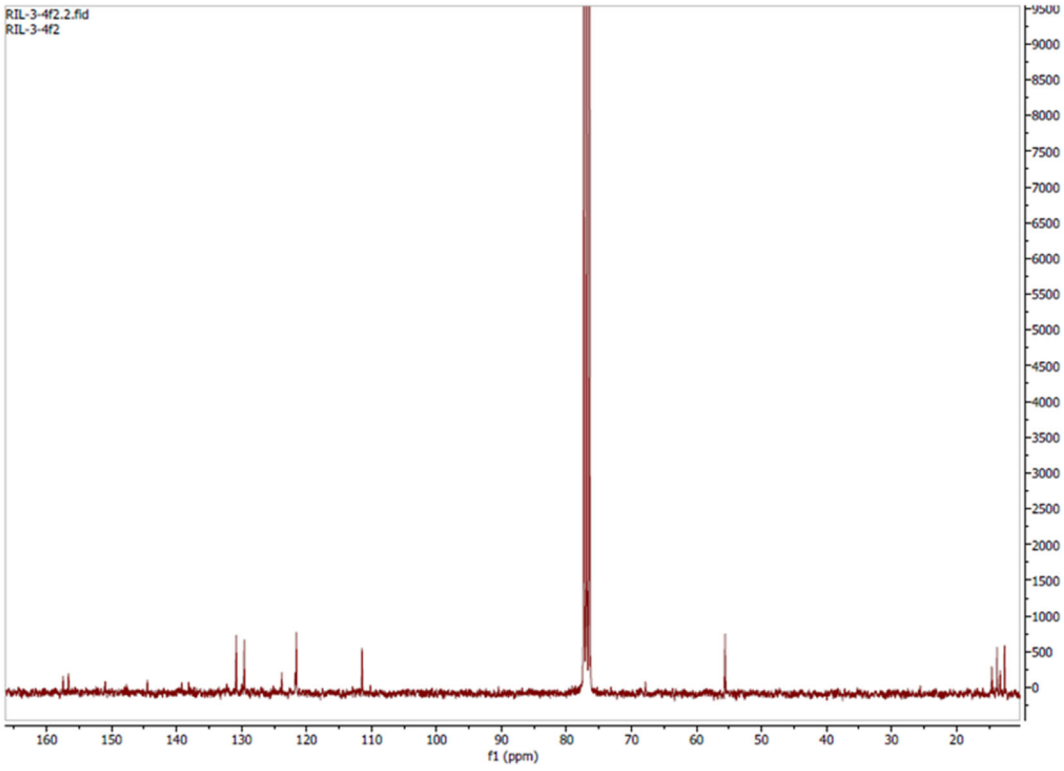
RIL-3-4f2.2.fid
RIL-3-4f2
f1 (ppm)

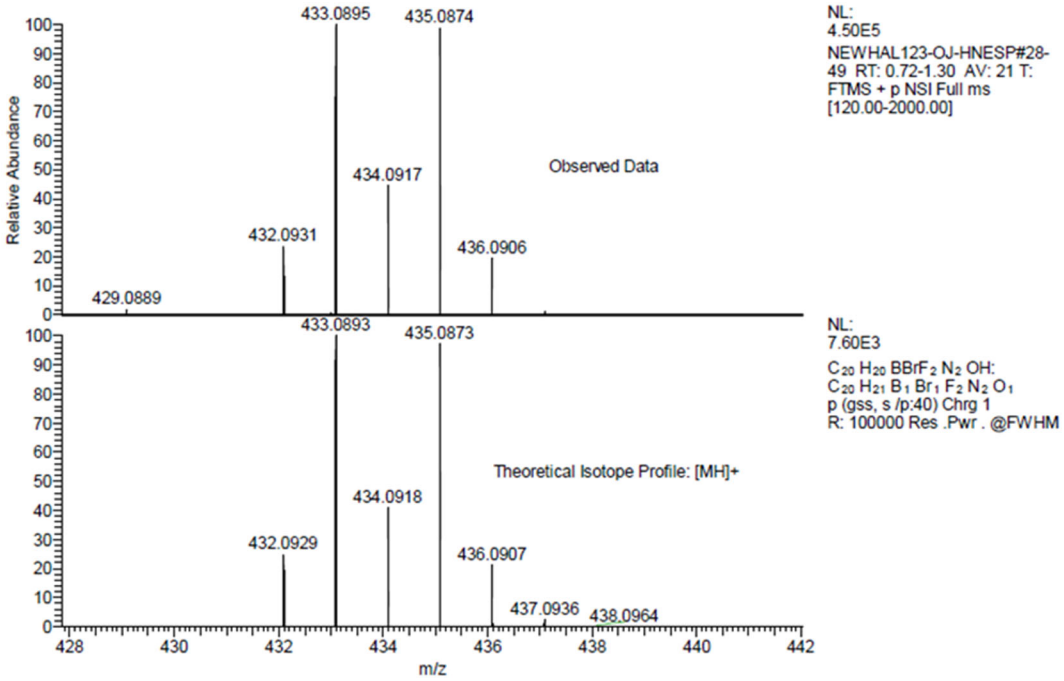
433.0895
435.0874
434.0917
432.0931
436.0906
429.0889
Observed Data
NL:
4.50E5
NEWHAL123-OJ-HNESP#28-49 RT: 0.72-1.30 AV: 21 T: FTMS + p NSI Full ms [120.00-2000.00]
433.0893
435.0873
434.0918
432.0929
436.0907
437.0936
438.0964
Theoretical Isotope Profile: [MH]+
NL:
7.60E3
C20 H20 BBrF2 N2 OH:
C20 H21 B1 Br1 F2 N2 O1
p (gss, s /p:40) Chrg 1
R: 100000 Res .Pwr . @FWHM
Relative Abundance
m/z

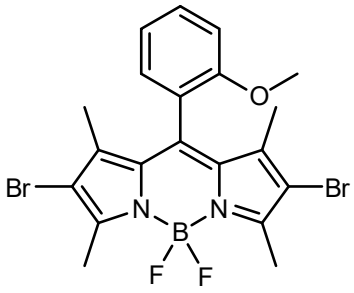
O
Br
N
B
N
Br
F
F

(BOD-6)

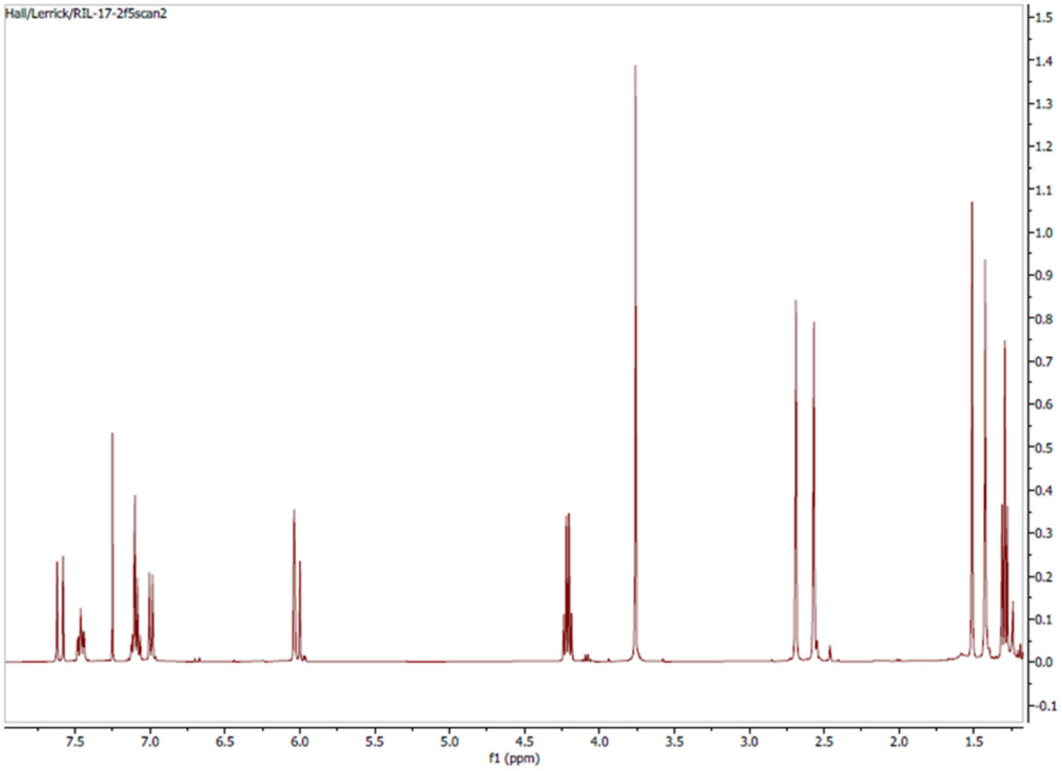
Hall/Lerrick/RIL-17-2f5scan2
7.5
7.0
6.5
6.0
5.5
5.0
4.5
4.0
3.5
3.0
2.5
2.0
1.5
f1 (ppm)

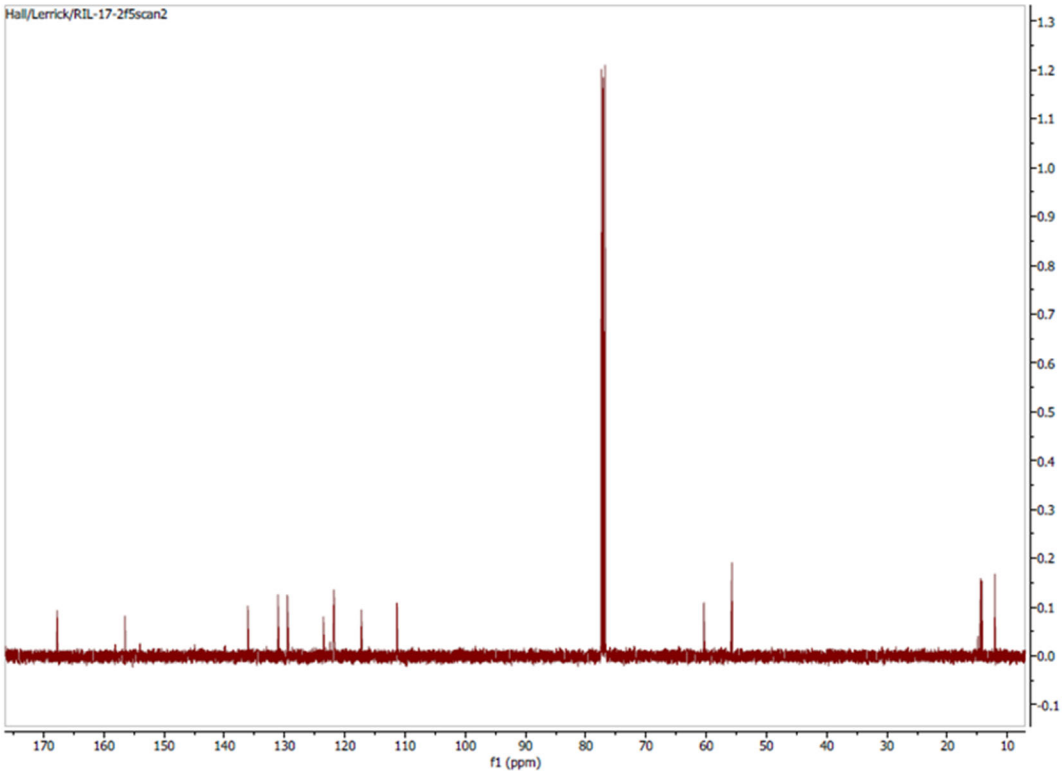
Hall/Lerrick/RIL-17-2f5scan2
f1 (ppm)

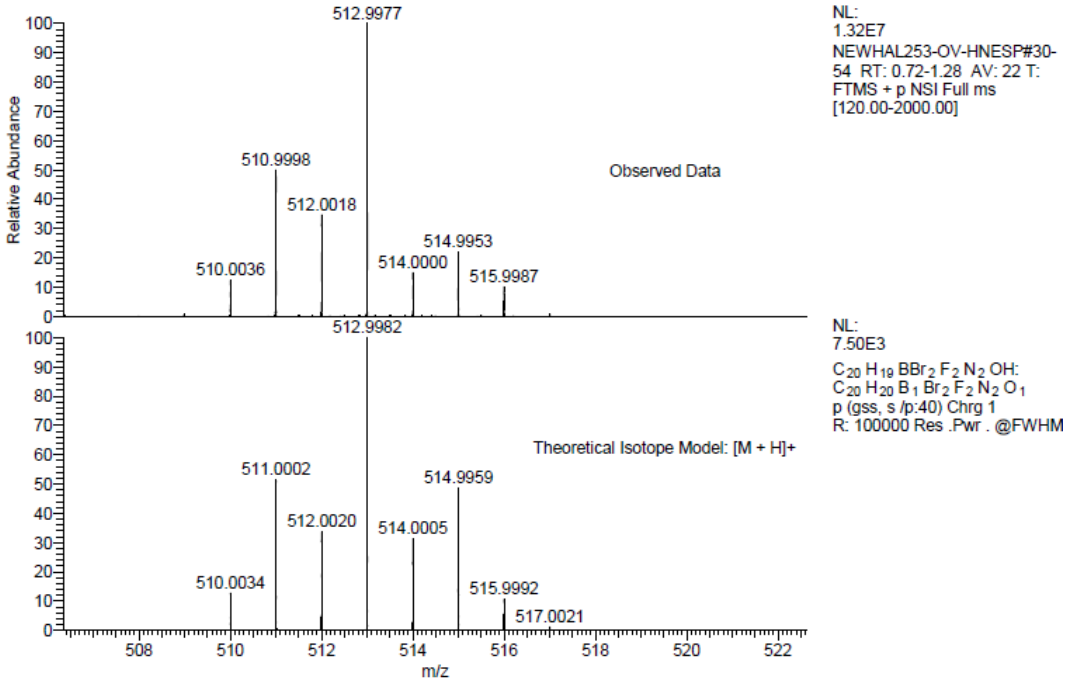
Relative Abundance
m/z
512.9977
510.9998
512.0018
510.0036
514.9953
514.0000
515.9987
Observed Data
NL:
1.32E7
NEWHAL253-OV-HNESP#30-54 RT: 0.72-1.28 AV: 22 T: FTMS + p NSI Full ms [120.00-2000.00]
512.9982
511.0002
512.0020
510.0034
514.9959
514.0005
515.9992
517.0021
Theoretical Isotope Model: [M + H]+
NL:
7.50E3
C20 H19 BBr2 F2 N2 OH:
C20 H20 B1 Br2 F2 N2 O1
p (gss, s /p:40) Chrg 1
R: 100000 Res .Pwr . @FWHM

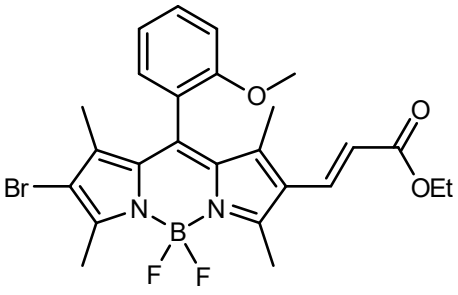
O
O
Br
N
N
B
F
F
OEt

(BOD-8)

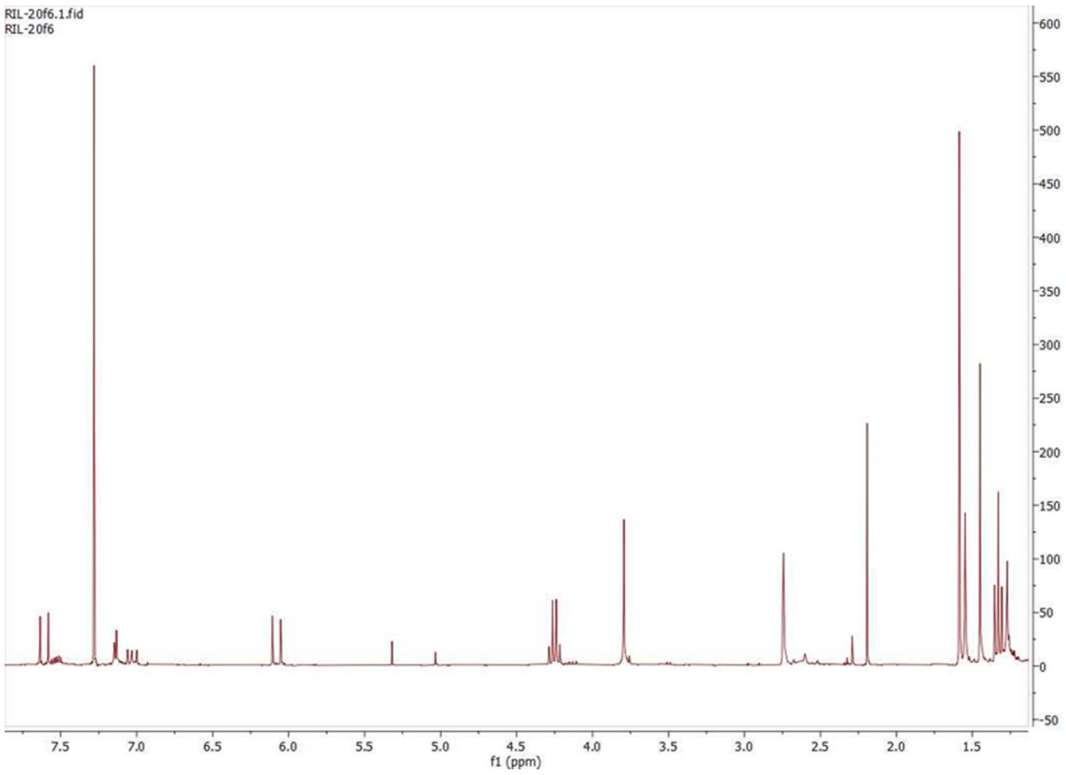
RIL-20f6.1.fid
RIL-20f6
600
550
500
450
400
350
300
250
200
150
100
50
0
-50
7.5
7.0
6.5
6.0
5.5
5.0
4.5
4.0
3.5
3.0
2.5
2.0
1.5
f1 (ppm)

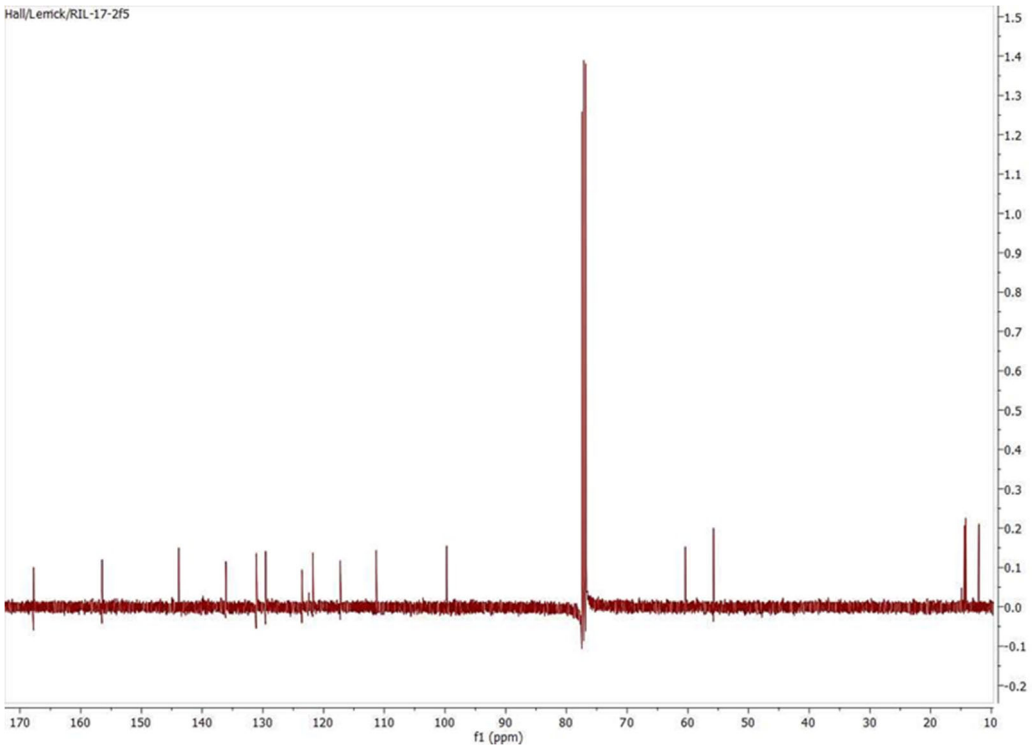
Hall/Lemick/RIL-17-2f5
1.5
1.4
1.3
1.2
1.1
1.0
0.9
0.8
0.7
0.6
0.5
0.4
0.3
0.2
0.1
0.0
-0.1
-0.2
170
160
150
140
130
120
110
100
90
80
70
60
50
40
30
20
10
f1 (ppm)

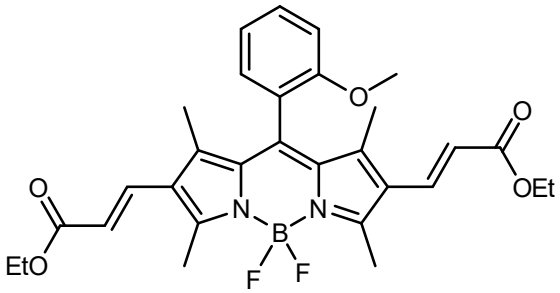
O
O
OEt
O
EtO
N
B
N
F
F

(BOD-9)

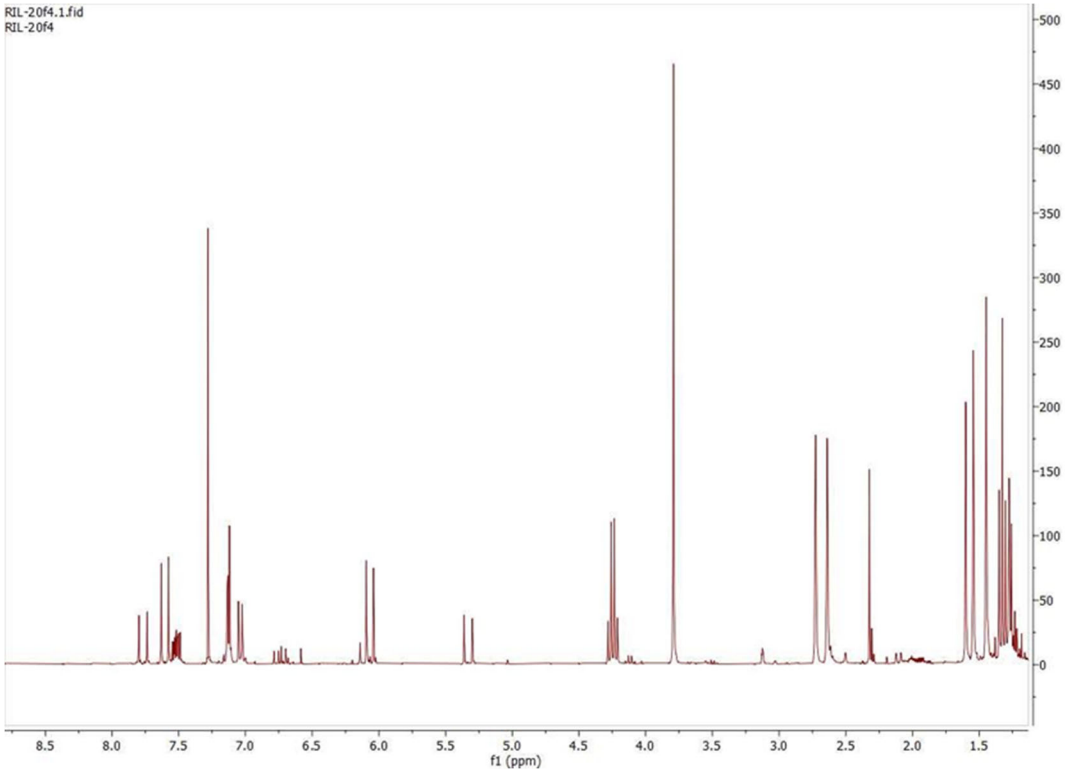
RIL-20f4.1.fid
RIL-20f4
500
450
400
350
300
250
200
150
100
50
0
8.5
8.0
7.5
7.0
6.5
6.0
5.5
5.0
4.5
4.0
3.5
3.0
2.5
2.0
1.5
f1 (ppm)

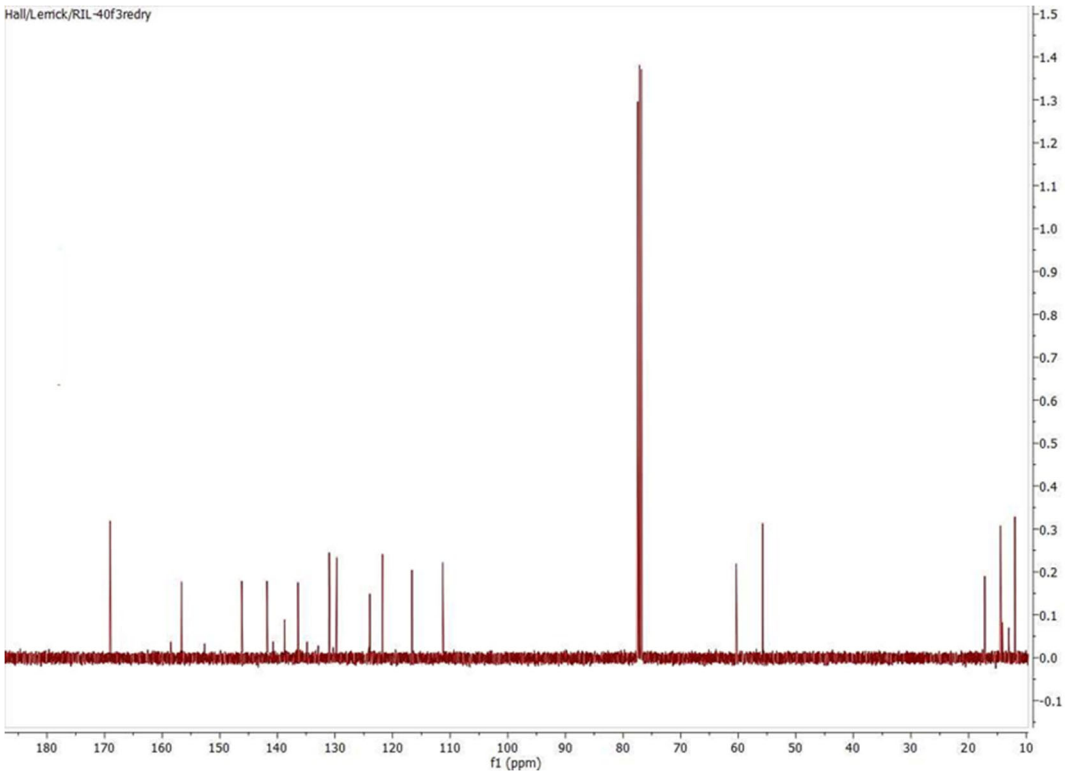

COMPUTATIONAL STUDY

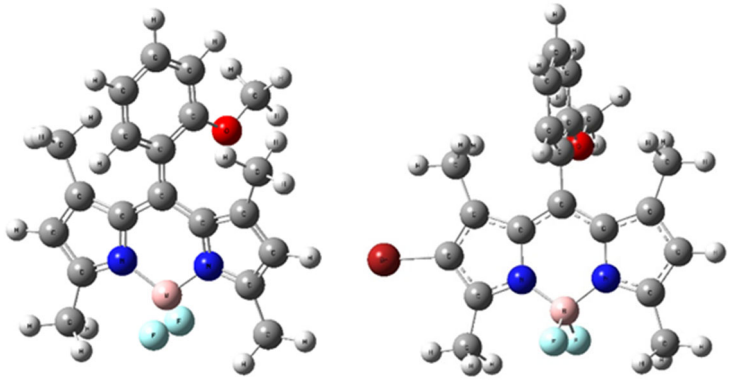

BOD-4 BOD-5

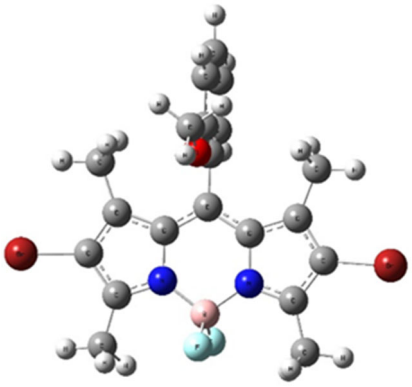

BOD-6

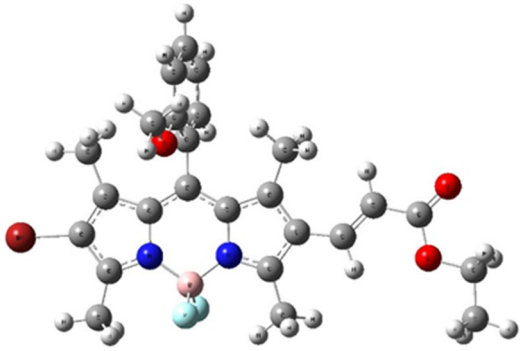

BOD-8

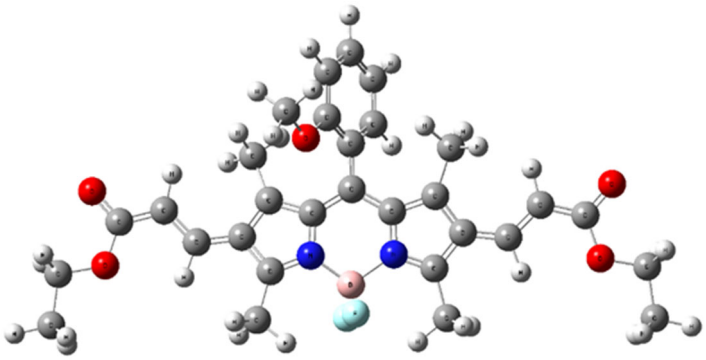

BOD-9

Table 1. The energy values, the MO energy of HOMO, LUMO levels, ΔE (in eV), and dipole moment μ (in Debye's) for BOD-4, 5, 6, 8, and 9

Quantity	BOD-4	BOD-5	BOD-6	BOD-8	BOD-9
Total energy (a.u.)	-1177.59	-1196.87	-1209.63	-1541.42	-1873.20
HOMO	-0.214 au	-0.210 au	-0.21696 au	-0.216 au	-0.21658 au
	(-5.82337 eV)	(-5.71431 eV)	(-5.90370 eV)	(-5.877576 eV)	(-5.893358eV)
LUMO	-0.095 au	-0.102 au	-0.1103 au	-0.113 au	-0.11595 au
	(-2.58514 eV)	(-2.775522 eV)	(-2.99321 eV)	(-3.074843 eV)	(-3.155115eV)
ΔE	3.23823 eV	2.938788 eV	2.91049 eV	2.802733 eV	2.738243 eV
M (Debye)	7.3033	8.0650	7.8595	5.7075	3.0751

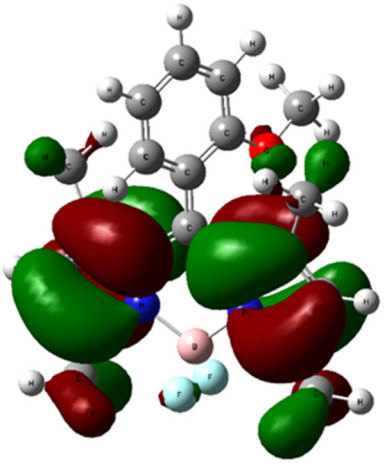

HOMO (BOD-4)

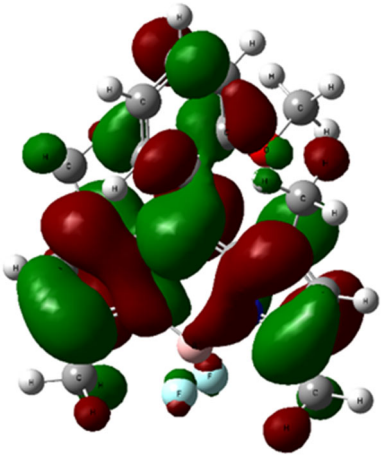

LUMO (BOD-4)

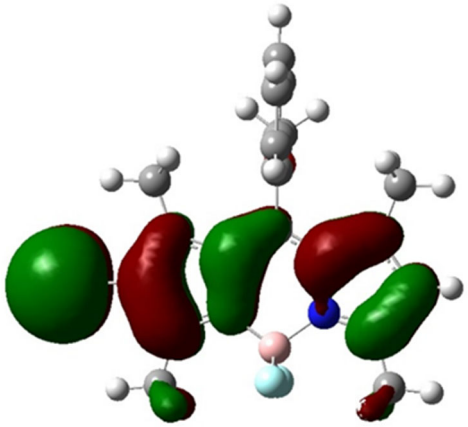

HOMO (BOD-5)

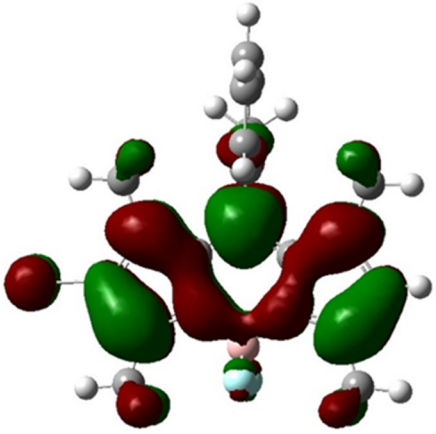

LUMO (BOD-5)

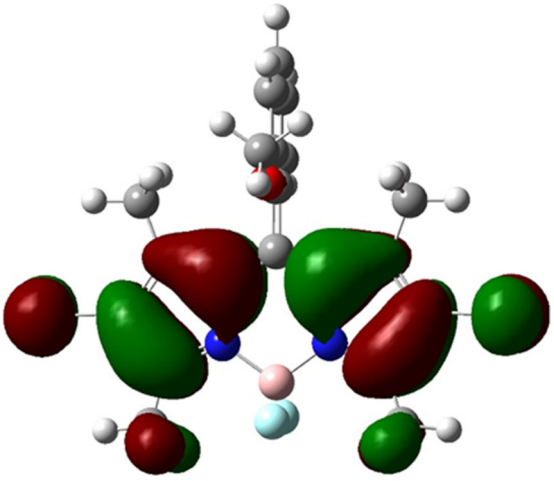

HOMO (BOD-6)

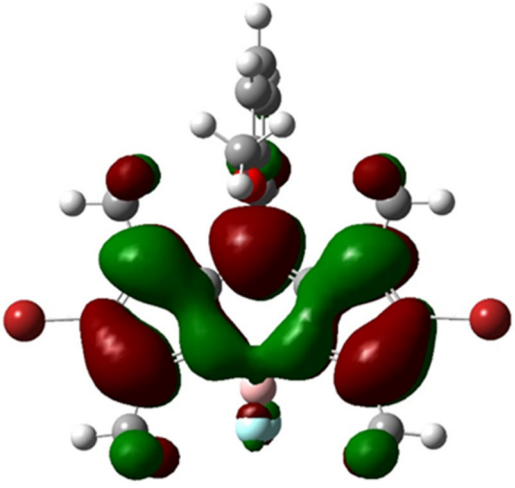

LUMO (BOD-6)

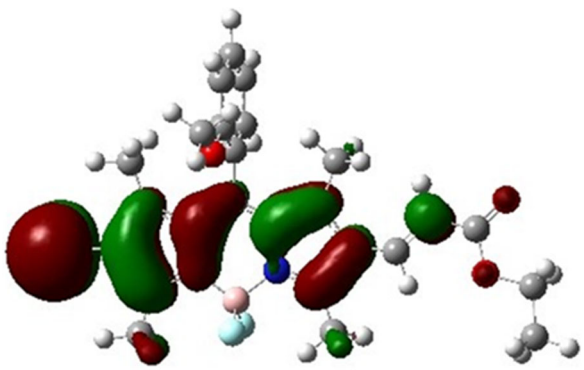

HOMO (BOD-8)

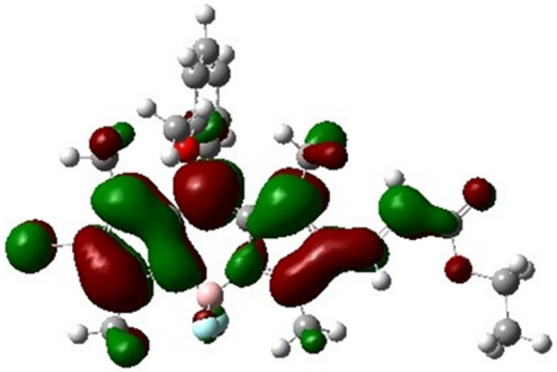

LUMO (BOD-8)

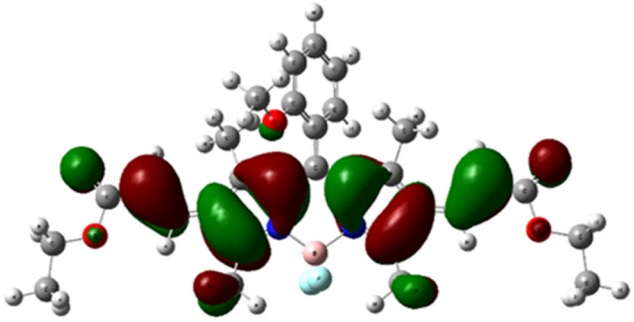

HOMO (BOD-9)

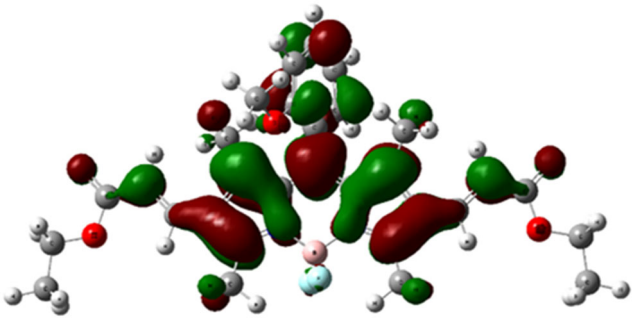

LUMO (BOD-9)